ARTICLE IN PRESS

Available online at www.sciencedirect.com

ScienceDirect

ELSEVIER

Chaos, Solitons and Fractals xxx (2006) xxx–xxx

CHAOS
SOLITONS & FRACTALS

www.elsevier.com/locate/chaos

Global bifurcations and chaotic dynamics for a string-beam coupled system

D.X. Cao, W. Zhang *

College of Mechanical Engineering, Beijing University of Technology, Beijing 100022, PR China

Accepted 20 September 2006

Communicated by Prof. M.S. El Naschie

Abstract

The global bifurcations and chaotic dynamics of a string-beam coupled system subjected to parametric and external excitations are investigated in detail in this paper. The governing equations are firstly obtained to describe the nonlinear transverse vibrations of the string-beam coupled system. The Galerkin procedure is introduced to simplify the governing equations of motion to ordinary differential equations with two-degrees-of-freedom. Using the method of multiple scales, parametrically and externally excited system is transformed to the averaged equation. The case of 1:2 internal resonance between the modes of the beam and string, principal parametric resonance for the beam and primary resonance for the string is considered. Based on the averaged equation, the theory of normal form is utilized to find the explicit formulas of normal form associated with one double zero and a pair of pure imaginary eigenvalues. The global perturbation method is employed to analyze the global bifurcations and chaotic dynamics of the string-beam coupled system. The analysis of the global bifurcations indicates that there exist the homoclinic bifurcations and the Silnikov type single-pulse homoclinic orbit in the averaged equation of the string-beam coupled system. These results obtained here mean that the chaotic motions can occur in the string-beam coupled system. Numerical simulations also verify the analytical predications.

1. Introduction

It is well known that research on nonlinear oscillations of the beam and string has received considerable attention because their importance in engineering applications, such as architecture, aircraft, mechanism, automobile and many others. However, there are many engineering systems can be reduced to a string-beam coupled model, for example, the optical fiber coupler used in telecommunications, cable-stayed bridge and tower crane and so on. In the past two decades, research on nonlinear dynamics of the string-beam coupled system has received little attention. Furthermore, the study on the global bifurcations and chaotic dynamics of the string-beam coupled system is much less. In this paper, we will study the global bifurcations and chaotic dynamics of a string-beam coupled system subjected to parametric and external excitations.

* Corresponding author.
E-mail addresses: cao_star@emails.bjut.edu.cn (D.X. Cao), sandyzhang0@yahoo.com (W. Zhang).

0960-0779/$ - see front matter © 2006 Elsevier Ltd. All rights reserved.
doi:10.1016/j.chaos.2006.09.072

It is necessary to mention the obtained achievements on research for the nonlinear oscillations of string-beam coupled structures. Cheng and Zu [1] proposed a string-beam coupled model with four nodes between the string and beam based on the optical fiber coupler. The analytical study and numerical simulation are carried out and the numerical results between the linear and nonlinear models are compared. Wang and Yang [2] used the finite element method to study the nonlinear dynamics of a cable-stayed bridge. Paolo et al. [3] found the dynamic characteristics of the Garigliano cable-stayed bridge in Italy using experimental method. They also compared the experimental results with those obtained from a finite element analysis. Fung et al. [4] used the Hamilton's principle to derive the governing equations of motion for a cable-stayed beam structure. They utilized numerical method to analyze the effect of the tension and the length of the cable. Ding [5,6] applied variation reduction method to study the periodic oscillations in a suspension bridge system and found that this system has at least period-3 oscillations. Gattulli et al. [7,8] studied the nonlinear interaction between the beam and cable in a cable-stayed bridge system and gave the experimental results. Cao and Zhang [9] used numerical method to study the nonlinear oscillations and chaotic dynamics of a string-beam coupled system with four-degrees-of- freedom.

The global bifurcations and chaotic dynamics for high-dimensional nonlinear systems are very important theoretical problem in science and engineering applications as they can reveal the instabilities of motion and complicated dynamical behaviors. The certain progress on the theories of the global bifurcations and chaotic dynamics for high- dimensional nonlinear systems has been obtained in the past two decades. Wiggins [10] divided four-dimensional perturbed Hamiltonian systems into three types and utilized the Melnikov method to investigate the global bifurcations and chaotic dynamics for these three basic systems. Kovacic and Wiggins [11] developed a new global perturbation technique to detect homoclinic and heteroclinic orbits in a class of four-dimensional ordinary differential equations. Later on, Kovacic [12] presented a constructive method which was a combination of the Melnikov method and geometric singular perturbation to prove the existence of transverse homoclinic orbits. Research given by Kaper and Kovacic [13] indicated the existence of multi-bump homoclinic orbits in near integrable Hamiltonian systems. Camassa et al. [14] presented an extension of the Melnikov method which could be used to analyze the existence of the multi-pulse homoclinic and heteroclinic orbits in a class of near-integrable Hamilton systems. In addition, Haller and Wiggins [15] combined the higher-dimensional Melnikov method, geometric singular perturbation theory and transversal theory to develop an energy-phase method. They studied the existence of homoclinic and heteroclinic orbits in a class of near integrable Hamiltonian systems. Haller [16] summarized the energy-phase method and presented detailed procedure of application to problems in mechanics.

Recently, researches on applying the theory of the global bifurcations and chaotic dynamics to engineering problems have been done by many researchers. Feng and Sethna [17] used the global perturbation method to study the global bifurcations and chaotic dynamics of thin plate under parametric excitation and obtained the conditions in which the Silnikov type homoclinic orbits and chaos can occur. Malhotra and Sri Namachchivaya [18,19] investigated the global dynamics of a shallow arch structure by using higher- dimensional Melnikov perturbation method and found that there exist Silnikov type homoclinic orbits. Feng and Liew [20] analyzed the existence of Silnikov homoclinic orbits in a perturbed mechanical system by using the global perturbation method. Malhotra et al. [21] used the energy-phase method to study the chaotic dynamics and the multi-pulse homoclinic orbits in the oscillations of flexible spinning discs. The global bifurcations and chaotic dynamics were investigated by Zhang [22] for parametrically excited simply supported rectangular thin plates. Zhang and Li [23] employed the global perturbation method to investigate the global bifurcations and chaotic dynamics of a nonlinear vibration absorber. The global bifurcations and chaotic dynamics for the nonlinear nonplanar oscillations of a cantilever beam were also studied by Zhang et al. [24]. Recently, Zhang and Yao [25] utilized the energy-phase method to analyze the Shilnikov type multi-pulse chaotic motions of a parametrically excited viscoelastic moving belt. Zhang et al. [26] analyzed multi-pulse chaotic motions of a rotor-active magnetic bearing system with time-varying stiffness. In [27], Zhang et al. used the global perturbation method to study global bifurcations and chaotic dynamics for a rotor-active magnetic bearing system with time-varying stiffness.

This paper is organized as follows. In Section 2 the governing equations of motion for the nonlinear transverse vibrations of the string-beam coupled system are given. The perturbation analysis using the method of multiple scales is finished in this section. The case of 1:2 internal resonance between the modes of the beam and string, principal parametric resonance for the beam and primary resonance for the string is considered. In Section 3 utilizing an improved adjoint operator method and the corresponding Maple program given by Zhang et al. [28], we obtain normal form of the averaged equation for the string-beam coupled system. In Section 4 based on the aforementioned research, the dynamics of the decoupled system is studied. In Section 5 the global analysis of the perturbed system is given. In Section 6 the higher-dimensional Melnikov theory is employed to determine the existence of the Silnikov type single-pulse homoclinic orbit in the averaged equation of the string-beam coupled system. In Section 7 numerical simulations are given by using phase portrait and Poincare map to verify the analytical predications. Finally, the conclusions are given in Section 8.

2. Equations of motion and perturbation analysis

We investigate the nonlinear transverse vibrations of a string-beam coupled system, as shown in Fig. 1. The string and beam are rigidly connected at each end point. The beam is subjected to a harmonic axial load at each end. The harmonic axial excitation may be expressed in the form $P = P_0 - F_2 \cos \Omega_2 t$. The string is pre-tensed at the two ends. The string-beam coupled system is simultaneously subjected to a fundamental vibration, which can be represented by $y_s = F_1 \cos \Omega_1 t$. We assume that the beam and string under consideration are homogeneous. The shear deformation and rotary inertia of the beam are neglected. In addition, the string and beam only have the transverse oscillations in the xoy plane, respectively. Furthermore, there is a very small distance between the beam and string to guarantee that they do not impact each other when transverse oscillations occur, as shown in Fig. 1(b).

It is thought that the string affects the axial load of the beam and, simultaneously, the beam does not influence the axial load of the string because the string is only subjected to the tension. Therefore, the coupling between the beam and string is performed by the two ends.

Based on the above assumptions, the governing equations of motion for the string-beam coupled system are obtained as follows:

$$m_1 \frac{\partial^2 w_1}{\partial t^2} + EI \frac{\partial^4 w_1}{\partial x^4} + c_1 \frac{\partial w_1}{\partial t} - \left\{ P_0 - F_2 \cos \Omega_2 t \right.$$
$$\left. + \frac{EA}{2l} \int_0^l \left(\frac{\partial w_1}{\partial x} \right)^2 \mathrm{d}x + \left[T_0 + \frac{K_s}{2} \int_0^l \left(\frac{\partial w_2}{\partial x} \right)^2 \mathrm{d}x \right] \right\} \frac{\partial^2 w_1}{\partial x^2} = m_1 F_1 \cos \Omega_1 t, \tag{1a}$$

$$m_2 \frac{\partial^2 w_2}{\partial t^2} + c_2 \frac{\partial w_2}{\partial t} - \left[T_0 + \frac{K_s}{2} \int_0^l \left(\frac{\partial w_2}{\partial x} \right)^2 \mathrm{d}x \right] \frac{\partial^2 w_2}{\partial x^2} = m_2 F_1 \cos \Omega_1 t, \tag{1b}$$

where the symbols m_1 and m_2 are the mass per unit length of the beam and string, respectively, w_1 and w_2 respectively denote the transverse deflection of the beam and string, l is the length of the beam and string, P_0 is the static, axial and compressive load, T_0 is the initial tension of the string, A and I are the area and moment of inertia of the cross section of the beam, c_1 and c_2 are the damping coefficients of the beam and string, K_s is the elastic coefficient of the string, E is Young's modulus of the beam.

The boundary conditions of the beam and string can be written as

$$\begin{aligned}
&\text{for beam}: \quad \text{at } x = 0, \quad \frac{\partial^2 w_1}{\partial x^2} = 0, \quad EI \frac{\partial^3 w_1}{\partial x^3} = -K w_1(0, t), \\
&\qquad\qquad\quad \text{at } x = l, \quad \frac{\partial^2 w_1}{\partial x^2} = 0, \quad EI \frac{\partial^3 w_1}{\partial x^3} = K w_1(l, t); \\
&\text{for string}: \quad \text{at } x = 0, \quad w_2(0, t) = w_1(0, t), \quad \text{at } x = l, \quad w_2(l, t) = w_1(l, t).
\end{aligned}$$

We introduce non-dimensional variables as follows:

$$t^* = t\sqrt{\frac{T_0 l^2 + EI}{(m_1 + m_2) l^4}}, \quad x^* = \frac{x}{l}, \quad w_1^* = \frac{w_1}{l}, \quad w_2^* = \frac{w_2}{l}, \quad F_2^* = \frac{(m_1 + m_2) F_2 l^2}{m_1 (T_0 l^2 + EI)}, \quad F_1^* = \frac{(m_1 + m_2) F_0 l^3}{T_0 l^2 + EI},$$
$$\Omega_1^* = \Omega_1 \sqrt{\frac{(m_1 + m_2) l^4}{T_0 l^2 + EI}}, \quad \Omega_2^* = \Omega_2 \sqrt{\frac{(m_1 + m_2) l^4}{T_0 l^2 + EI}}. \tag{2}$$

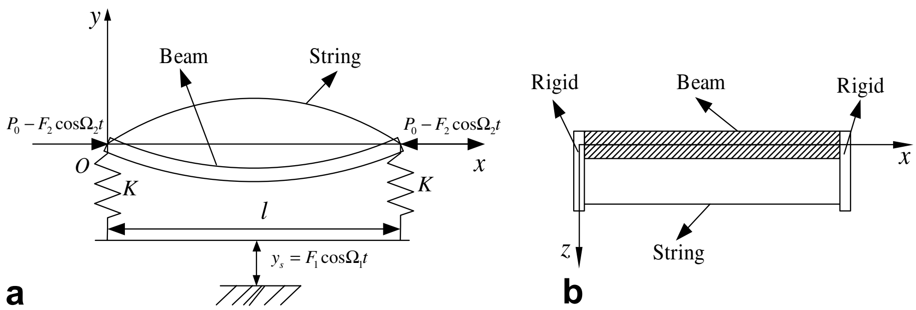

Fig. 1. The simplified model of a sting-beam coupled system: (a) the front view of the model and (b) the top view of the model.

Please cite this article in press as: Cao DX, Zhang W, Global bifurcations and chaotic dynamics ..., Chaos, Solitons & Fractals (2006), doi:10.1016/j.chaos.2006.09.072

Substituting Eq. (2) into Eq. (1) and dropping the asterisk, the final governing equations of motion in non-dimensional form are obtained as

$$\frac{\partial^2 w_1}{\partial t^2} + \mu_1 \frac{\partial w_1}{\partial t} + \beta_1 \frac{\partial^4 w_1}{\partial x^4} - \beta_2 \frac{\partial^2 w_1}{\partial x^2} + F_2 \cos(\Omega_2 t) \frac{\partial^2 w_1}{\partial x^2} - \beta_3 \int_0^l \left(\frac{\partial w_1}{\partial x}\right)^2 \mathrm{d}x \cdot \frac{\partial^2 w_1}{\partial x^2} - \beta_4 \int_0^l \left(\frac{\partial w_2}{\partial x}\right)^2 \mathrm{d}x \cdot \frac{\partial^2 w_1}{\partial x^2} = F_1 \cos(\Omega_1 t), \tag{3a}$$

$$\frac{\partial^2 w_2}{\partial t^2} + \mu_2 \frac{\partial w_2}{\partial t} - \alpha_1 \frac{\partial^2 w_2}{\partial x^2} - \alpha_2 \int_0^l \left(\frac{\partial w_2}{\partial x}\right)^2 \mathrm{d}x \cdot \frac{\partial^2 w_2}{\partial x^2} = F_1 \cos(\Omega_1 t), \tag{3b}$$

where

$$\mu_1 = \frac{c_1}{m_1}\sqrt{\frac{(m_1+m_2)l^4}{T_0 l^2 + EI}}, \quad \beta_1 = \frac{(m_1+m_2)EI}{m_1(T_0 l^2 + EI)}, \quad \beta_2 = \frac{(m_1+m_2)(P_0+T_0)l^2}{m_1(T_0 l^2 + EI)},$$
$$\beta_3 = \frac{(m_1+m_2)EAl^2}{2m_1(T_0 l^2 + EI)}, \quad \beta_4 = \frac{(m_1+m_2)K_s l^3}{2m_1(T_0 l^2 + EI)}, \quad \mu_2 = \frac{c_2}{m_2}\sqrt{\frac{(m_1+m_2)l^4}{T_0 l^2 + EI}},$$
$$\alpha_1 = \frac{(m_1+m_2)T_0 l^2}{m_2(T_0 l^2 + EI)}, \quad \alpha_2 = \frac{(m_1+m_2)K_s l^3}{2m_2(T_0 l^2 + EI)}.$$

Considering that the equations of motion for the string and beam are coupled, therefore, it is assumed that the mode of the string consists of the same spatial mode shape of the beam and another relative displacement with respect to the beam. To perform a single-mode Galerkin discretization, the transverse displacement w_1 and w_2 can be expressed as follows [1]:

$$w_1(x,t) = Y_1(x)y_1(t), \tag{4a}$$
$$w_2(x,t) = Y_2(x)y_2(t) + Y_1(x)y_1(t), \tag{4b}$$

where $y_1(t)$ is the displacement of the beam and $y_2(t)$ the relative displacement with respect to the beam.

The mode shapes are derived as

$$Y_1(x) = C_1[K_A \sin K^*x + \cos K^*x + K_C \sinh K^*x + \cosh K^*x], \tag{5a}$$
$$Y_2(x) = C_2 \sin\frac{\pi}{l}x, \tag{5b}$$

where

$$K_A = \frac{\cos K^*l - \cosh K^*x + 2K \sinh K^*l/(EIK^{*^3})}{\sinh K^*l - \sin K^*l},$$
$$K_C = \frac{cosK^*l - \cosh K^*x + 2K \sin K^*l/(EIK^{*^3})}{\sinh K^*l - \sin K^*l},$$

and K^* can be numerically obtained from the following equation:

$$EJK^{*3}(-K_A \cos K^*l + \sin K^*l + K_C \cosh K^*l + \sinh K^*l) - K(K_A \sin K^*l + \cos K^*l + K_C \sinh K^*l + \cosh K^*l) = 0. \tag{6}$$

Then, substituting Eq. (4) into Eq. (3) and applying single-mode Galerkin truncation to system (3), we can obtain the following nonlinear ordinary differential governing equations of motion for the string-beam coupled system under parametric and forcing excitation with two-degrees-of-freedom:

$$\ddot{y}_1 + \mu_1\dot{y}_1 + (\beta_1 K^{*4} - \beta_2 l_{11})y_1 + F_2 l_{11}\cos\Omega_2 t \cdot y_1 - (\beta_3 g_{11} l_{11} + \beta_4 g_{11} l_{11})y_1^3 - \beta_4 g_{22} l_{11} y_2^2 y_1 - 2\beta_4 g_{12} l_{11} y_2 y_1^2 = f_{11}\cos\Omega_1 t, \tag{7a}$$

$$\ddot{y}_2 + \lambda_{21}\ddot{y}_1 + \mu_2\dot{y}_2 + \mu_2\lambda_{21}\dot{y}_1 - \alpha_1 l_{22} y_2 - \alpha_1 l_{12} y_1 - \alpha_2 g_{22} l_{22} y_2^3 - \alpha_2(g_{22} l_{12} + 2g_{21} l_{22})y_2^2 y_1 - \alpha_2(g_{11} l_{22} + 2g_{21} l_{12})y_2 y_1^2 - \alpha_2 g_{11} l_{12} y_1^3 = f_{12}\cos\Omega_1 t, \tag{7b}$$

where

$$\lambda_{mn} = \int_0^l Y_m(x)Y_n(x)\,\mathrm{d}x, \quad g_{mn} = \int_0^l Y'_m(x)Y'_n(x)\,\mathrm{d}x,$$
$$l_{mn} = \int_0^l Y''_m(x)Y_n(x)\,\mathrm{d}x, \quad f_{1m} = \int_0^l F_1(x)Y_m(x)\,\mathrm{d}x, \qquad m,n = 1,2.$$

To obtain a system which is suitable to use the method of multiple scales [29], the scale transformations are introduced. Then, system (7) can be rewritten as

$$\ddot{y}_1 + \varepsilon\mu_1\dot{y}_1 + (\omega_1^2 + \varepsilon f_2 \cos\Omega_2 t)y_1 - \varepsilon a_{11}y_1y_2^2 - \varepsilon a_{13}y_1^2y_2 - \varepsilon a_{14}y_1^3 = \varepsilon f_{11}\cos\Omega_1 t, \tag{8a}$$

$$\ddot{y}_2 + \varepsilon b_{21}\ddot{y}_1 + \varepsilon\mu_2\dot{y}_2 + \varepsilon b_{22}\dot{y}_1 + \omega_2^2 y_2 - \varepsilon b_{23}y_1 - \varepsilon a_{21}y_2^3 - \varepsilon a_{22}y_1y_2^2 - \varepsilon a_{23}y_1^2y_2 - \varepsilon a_{24}y_1^3 = \varepsilon f_{12}\cos\Omega_1 t, \tag{8b}$$

where ε is a small perturbation parameter and

$$\omega_1^2 = \beta_1 K^{*4} - \beta_2 l_{11},\quad f_2 = F_2 l_{11},\quad a_{11} = \beta_4 g_{22} l_{11},\quad a_{13} = 2\beta_4 g_{12} l_{11},$$
$$a_{14} = \beta_3 g_{11} l_{11} + \beta_4 g_{11} l_{11},\quad b_{21} = \lambda_{21},\quad b_{22} = \mu_2\lambda_{21},\quad \omega_2^2 = -\alpha_1 l_{22},\quad b_{23} = \alpha_1 l_{12},$$
$$a_{21} = \alpha_2 g_{22} l_{22},\quad a_{22} = \alpha_2(g_{22}l_{12} + 2g_{21}l_{22}),\quad a_{23} = \alpha_2(g_{11}l_{22} + 2g_{21}l_{12}),\quad a_{24} = \alpha_2 g_{11} l_{12}.$$

In the following analysis, the method of multiple scales is used to determine the uniform solution of Eq. 8. We introduce the two time scales $T_0 = t$ and $T_1 = \varepsilon t$ and expand the time-dependent variable y_n $(n = 1, 2)$ as

$$y_n(t) = y_{n0}(T_0, T_1) + \varepsilon y_{n1}(T_0, T_1) + \cdots,\quad (n = 1, 2). \tag{9}$$

Then, we have the differential operators

$$\frac{\mathrm{d}}{\mathrm{d}t} = \frac{\partial}{\partial T_0}\frac{\partial T_0}{\partial t} + \frac{\partial}{\partial T_1}\frac{\partial T_1}{\partial t} + \cdots = D_0 + \varepsilon D_1 + \cdots, \tag{10a}$$

$$\frac{\mathrm{d}^2}{\mathrm{d}t^2} = (D_0 + \varepsilon D_1 + \cdots)^2 = D_0^2 + 2\varepsilon D_0 D_1 + \cdots, \tag{10b}$$

where $D_k = \partial/\partial T_k$ $(k = 0, 1)$.

Fig. 2 indicates the relationship between two times first-order natural frequency of the string and the first-order natural frequency of the beam with the initial tension T_0. It is noticed that there exists 1:2 internal resonance between the first order modes of the beam and string when $T_0 \approx 0.2693$. In addition, principal parametric resonance for the beam and primary resonance for the string are considered. The resonant relations are represented as

$$\omega_1 = 2\omega_2,\quad \omega_1^2 = \frac{1}{4}\Omega_2^2 + \varepsilon\sigma_1,\quad \omega_2^2 = \frac{1}{16}\Omega_2^2 + \varepsilon\sigma_2,\quad \Omega_1 = \frac{1}{4}\Omega_2, \tag{11}$$

where σ_1 and σ_2 are two detuning parameters. For convenience of the following analysis, we let $\Omega_2 = 1$.

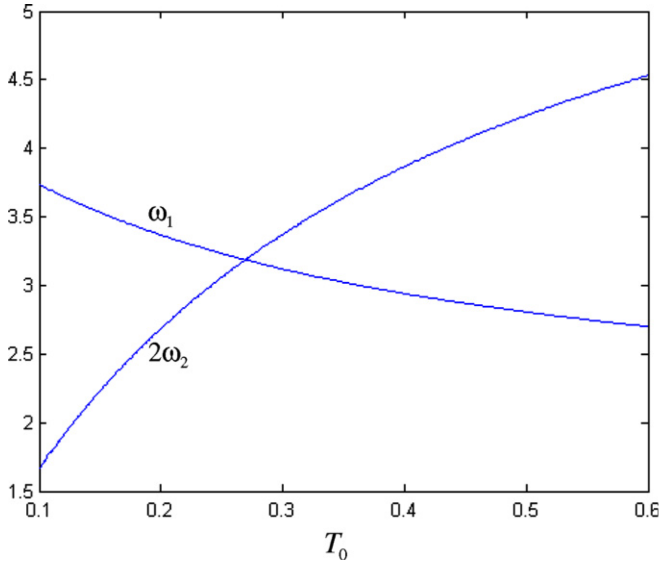

Fig. 2. The relationship between two times first-order natural frequency of the string and the first-order natural frequency of the beam with the initial tension T_0.

Substituting Eq. (9)–(11) into Eq. (8), and balancing the coefficients of like power of ε on the left hand side and the right hand side yield the following differential equations
order ε^0:

$$D_0^2 y_{10} + \frac{1}{4}\Omega_2^2 y_{10} = 0, \tag{12a}$$

$$D_0^2 y_{20} + \frac{1}{16}\Omega_2^2 y_{20} = 0, \tag{12b}$$

order ε^1

$$D_0^2 y_{11} + \frac{1}{4}\Omega_2^2 y_{11} = -2D_0 D_1 y_{10} - \mu_1 D_0 y_{10} - \sigma_1 y_{10} - f_2 y_{10}\cos\Omega_2 t + a_{11} y_{10} y_{20}^2 + a_{13} y_{10}^2 y_{20} + a_{14} y_{10}^3 + f_{11}\cos\left(\frac{1}{4}\Omega_2\right)t, \tag{13a}$$

$$D_0^2 y_{21} + \frac{1}{16}\Omega_2^2 y_{21} = -2D_0 D_1 y_{20} - b_{21} D_0^2 y_{10} - \mu_2 D_0 y_{20} - b_{22} D_0 y_{10} - \sigma_2 y_{20} + b_{23} y_{10} + a_{21} y_{20}^3 + a_{22} y_{10} y_{20}^2 + a_{23} y_{10}^2 y_{20} + a_{24} y_{10}^3 + f_{12}\cos\left(\frac{1}{4}\Omega_2\right)t. \tag{13b}$$

The solutions of Eq. (12) can be expressed as

$$y_{10} = A_1(T_1)e^{\frac{i}{2}\Omega_2 T_0} + \bar{A}_1(T_1)e^{-\frac{i}{2}\Omega_2 T_0}, \tag{14a}$$

$$y_{20} = A_2(T_1)e^{\frac{i}{4}\Omega_2 T_0} + \bar{A}_2(T_1)e^{-\frac{i}{4}\Omega_2 T_0}, \tag{14b}$$

where $\overline{A}_1$ and $\overline{A}_2$ are the parts of the complex conjugate of A_1 and A_2, respectively.
Substituting Eq. (14) into Eq. (13) yields

$$D_0^2 y_{11} + \frac{1}{4}\Omega_2^2 y_{11} = \left[-i\Omega_2 D_1 A_1 - \frac{1}{2} i\mu_1 \Omega_2 A_1 - \sigma_1 A_1 - \frac{1}{2} f_2 \overline{A}_1 + 2a_{11} A_1 A_2 \overline{A}_2 + 3a_{14} A_1^2 \overline{A}_1\right] e^{i\frac{1}{2}\Omega_2 T_0} + cc + NST, \tag{15a}$$

$$D_0^2 y_{21} + \frac{1}{16}\Omega_2^2 y_{21} = \left[-\frac{i}{2}\Omega_2 D_1 A_2 - \frac{i}{4}\mu_2 \Omega_2 A_2 - \sigma_2 A_2 + 3a_{21} A_2^2 \overline{A}_2 + 2a_{23} A_1 \overline{A}_1 A_2 + \frac{1}{2} f_{12}\right] e^{i\frac{1}{4}\Omega_2 T_0} + cc + NST, \tag{15b}$$

where the symbol cc and NST respectively denote the parts of the complex conjugate of the functions on the right hand side of Eq. (15) and the non-secular terms.

Eliminating the terms that produce secular terms from Eq. (15), we obtain the following averaged equation in complex form:

$$D_1 A_1 = -\frac{1}{2}\mu_1 A_1 + \frac{i}{\Omega_2}\sigma_1 A_1 + \frac{i}{2\Omega_2} f_2 \overline{A}_1 - \frac{2i}{\Omega_2} a_{11} A_1 A_2 \overline{A}_2 - \frac{3i}{\Omega_2} a_{14} A_1^2 \overline{A}_1, \tag{16a}$$

$$D_1 A_2 = -\frac{1}{2}\mu_2 A_2 + \frac{2i}{\Omega_2}\sigma_2 A_2 - \frac{6}{\Omega_2} a_{21} A_2^2 \overline{A}_2 - \frac{4a_{23}}{\Omega_2} A_1 \overline{A}_1 A_2 + \frac{i}{\Omega_2} f_{12}. \tag{16b}$$

The functions A_k $(k = 1, 2)$ may be denoted in the Cartesian form

$$A_1 = x_1 + ix_2, \quad A_2 = x_3 + ix_4. \tag{17}$$

Substituting Eq. (17) into Eq. (16), separating the real and imaginary parts and solving for dx_i/dT_1 $(i = 1, 2, 3, 4)$ from the resulting equations, four-dimensional nonlinear averaged equation in the Cartesian form is obtained as follows:

$$\dot{x}_1 = -\frac{1}{2}\mu_1 x_1 - \sigma_1 x_2 + \frac{1}{2} f_2 x_2 + 2a_{11}(x_3^2 + x_4^2)x_2 + 3a_{14}(x_1^2 + x_2^2)x_2, \tag{18a}$$

$$\dot{x}_2 = -\frac{1}{2}\mu_1 x_2 + \sigma_1 x_1 + \frac{1}{2} f_2 x_1 - 2a_{11}(x_3^2 + x_4^2)x_1 - 3a_{14}(x_1^2 + x_2^2)x_1, \tag{18b}$$

$$\dot{x}_3 = -\frac{1}{2}\mu_2 x_3 - 2\sigma_2 x_4 + 6a_{21}(x_3^2 + x_4^2)x_4 + 4a_{23}(x_1^2 + x_2^2)x_4, \tag{18c}$$

$$\dot{x}_4 = -\frac{1}{2}\mu_2 x_4 + 2\sigma_2 x_3 - 6a_{21}(x_3^2 + x_4^2)x_3 - 4a_{23}(x_1^2 + x_2^2)x_3 - f_{12}. \tag{18d}$$

3. Computation of normal form

In order to conveniently analyze the global bifurcations and chaotic dynamics of the string-beam coupled system, it is necessary to reduce averaged Eq. (18) to a simpler normal form. In this section, an improved adjoint operator method and the corresponding Maple program given by Zhang et al. [28] will be utilized to obtain normal form of averaged Eq. (18) for the string-beam coupled system.

It is obviously seen that there exist $Z_2 \oplus Z_2$ and D_4 symmetries in averaged Eq. (18) without the parameters. Consequently, these symmetries are also held in normal form. Take into account the exciting amplitude f_{12} as a perturbation parameter. Amplitude f_{12} can be considered as an unfolding parameter when the global bifurcations are investigated.

It is noticed that Eq. (18) without the perturbation parameter f_{12} has obviously a trivial zero solution $(y_1, y_2, y_3, y_4) = (0,0,0,0)$ at which the Jacobian matrix can be written as

$$J = \begin{bmatrix} -\frac{1}{2}\mu_1 & -\sigma_1 + \frac{1}{2}f_2 & 0 & 0 \\ \sigma_1 + \frac{1}{2}f_2 & -\frac{1}{2}\mu_1 & 0 & 0 \\ 0 & 0 & -\frac{1}{2}\mu_2 & -2\sigma_2 \\ 0 & 0 & 2\sigma_2 & -\frac{1}{2}\mu_2 \end{bmatrix}. \tag{19}$$

The characteristic equation corresponding to the trivial zero solution is of the form

$$\left(\lambda^2 + \mu_1\lambda + \Delta_1\right)\left(\lambda^2 + \mu_2\lambda + \Delta_2\right) = 0. \tag{20}$$

where $\Delta_1 = \sigma_1^2 + \frac{1}{4}\mu_1^2 - \frac{1}{4}f_2^2$, $\Delta_2 = \frac{1}{4}\mu_2^2 + 4\sigma_2^2$.

When $\mu_1 = \mu_2 = 0$ and $\Delta_1 = 0$ are simultaneously satisfied, system (18) without the perturbation parameter f_{12} has one non-semisimple double zero and a pair of pure imaginary eigenvalues

$$\lambda_{1,2} = 0, \quad \lambda_{3,4} = \pm \mathrm{i}\bar{\omega}, \tag{21}$$

where $\bar{\omega}^2 = 4\sigma_2^2$.

Let $\sigma_1 = \bar{\sigma}_1 - f_2/2$ as well as $f_2 = 1$. Considering $\bar{\sigma}_1, f_2, \mu_1$ and μ_2 as the perturbation parameters, then, averaged Eq. (18) without the perturbation parameters is changed to the following form:

$$\dot{x}_1 = x_2 + 2a_{11}(x_3^2 + x_4^2)x_2 + 3a_{14}(x_1^2 + x_2^2)x_2, \tag{22a}$$
$$\dot{x}_2 = -2a_{11}(x_3^2 + x_4^2)x_1 - 3a_{14}(x_1^2 + x_2^2)x_1, \tag{22b}$$
$$\dot{x}_3 = -2\sigma_2 x_4 + 6a_{21}(x_3^2 + x_4^2)x_4 + 4a_{23}(x_1^2 + x_2^2)x_4, \tag{22c}$$
$$\dot{x}_4 = 2\sigma_2 x_3 - 6a_{21}(x_3^2 + x_4^2)x_3 - 4a_{23}(x_1^2 + x_2^2)x_3. \tag{22d}$$

Thus, the Jacobian matrix of Eq. (22) is written as follows:

$$A = \begin{bmatrix} 0 & 1 & 0 & 0 \\ 0 & 0 & 0 & 0 \\ 0 & 0 & 0 & -2\sigma_2 \\ 0 & 0 & 2\sigma_2 & 0 \end{bmatrix}. \tag{23}$$

Using an improved adjoint operator method and the corresponding Maple program given by Zhang et al. [28], 3-order normal form of the averaged equation for the string-beam coupled system is obtained as

$$\dot{x}_1 = x_2, \tag{24a}$$
$$\dot{x}_2 = -3a_{14}x_1^3 - 2a_{11}x_1x_3^2 - 2a_{11}x_1x_4^2, \tag{24b}$$
$$\dot{x}_3 = -2\sigma_2 x_4 + 6a_{21}x_4^3 + 4a_{23}x_1^2x_4 + 6a_{21}x_3^2x_4, \tag{24c}$$
$$\dot{x}_4 = 2\sigma_2 x_3 - 6a_{21}x_3^3 - 4a_{23}x_1^2x_3 - 6a_{21}x_3x_4^2. \tag{24d}$$

Normal form with perturbation parameters for the string-beam coupled system can be written as

$$\dot{x}_1 = -\bar{\mu}_1 x_1 + (1 - \bar{\sigma}_1)x_2, \tag{25a}$$
$$\dot{x}_2 = \bar{\sigma}_1 x_1 - \bar{\mu}_1 x_2 - 3a_{14}x_1^3 - 2a_{11}x_1x_3^2 - 2a_{11}x_1x_4^2, \tag{25b}$$
$$\dot{x}_3 = -\bar{\mu}_2 x_3 - \bar{\sigma}_2 x_4 + 6a_{21}x_4^3 + 4a_{23}x_1^2x_4 + 6a_{21}x_3^2x_4, \tag{25c}$$
$$\dot{x}_4 = \bar{\sigma}_2 x_3 - \bar{\mu}_2 x_4 - 6a_{21}x_3^3 - 4a_{23}x_1^2x_3 - 6a_{21}x_3x_4^2 - f_{12}, \tag{25d}$$

where $\bar{\mu}_1 = \mu_1/2$, $\bar{\mu}_2 = \mu_2/2$, $\bar{\sigma}_2 = 2\sigma_2$.

Please cite this article in press as: Cao DX, Zhang W, Global bifurcations and chaotic dynamics ..., Chaos, Solitons & Fractals (2006), doi:10.1016/j.chaos.2006.09.072

Further, we let

$$x_3 = I\cos\gamma, \quad x_4 = I\sin\gamma. \tag{26}$$

Substituting Eq. (26) into Eq. (25), we obtain the following equation:

$$\dot{x}_1 = -\bar{\mu}_1 x_1 + (1-\bar{\sigma}_1)x_2, \tag{27a}$$
$$\dot{x}_2 = \bar{\sigma}_1 x_1 - \bar{\mu}_1 x_2 - 3a_{14}x_1^3 - 2a_{11}x_1 I^2, \tag{27b}$$
$$\dot{I} = -\bar{\mu}_2 I - f_{12}\sin\gamma, \tag{27c}$$
$$I\dot{\gamma} = \bar{\sigma}_2 I - 6a_{21}I^3 - 4a_{23}x_1^2 I - f_{12}\cos\gamma. \tag{27d}$$

In order to get the unfolding of Eq. (27), a linear transformation is introduced as

$$\begin{bmatrix} x_1 \\ x_2 \end{bmatrix} = \sqrt{\frac{|a_{11}|}{2|a_{23}|}}\begin{bmatrix} 1-\bar{\sigma}_1 & 0 \\ \bar{\mu}_1 & 1 \end{bmatrix}\begin{bmatrix} u_1 \\ u_2 \end{bmatrix}. \tag{28}$$

Substituting Eq. (28) into Eq. (27) and canceling nonlinear terms which include the parameter $\bar{\sigma}_1$ yield the unfolding as follows:

$$\dot{u}_1 = u_2, \tag{29a}$$
$$\dot{u}_2 = c_1 u_1 - c_2 u_2 - \alpha_1 u_1^3 - \beta_1 u_1 I^2, \tag{29b}$$
$$\dot{I} = -c_3 I - f_{12}\sin\gamma, \tag{29c}$$
$$I\dot{\gamma} = \bar{\sigma}_2 I - \alpha_2 I^3 - \beta_1 u_1^2 I - f_{12}\cos\gamma, \tag{29d}$$

where

$$c_1 = -\bar{\mu}_1^2 + \bar{\sigma}_1(1-\bar{\sigma}_1), \quad c_2 = 2\mu_1, \quad \alpha_1 = 6a_{14}a_{11}/a_{23}, \quad \beta_1 = 2a_{11}, \quad c_3 = \bar{\mu}_2, \quad \alpha_2 = 6a_{21}.$$

Introduce the following scale transformations $c_2 \to \varepsilon c_2$, $c_3 \to \varepsilon c_3$, $\bar{f}_{12} \to \varepsilon \bar{f}_{12}$. Then, unfolding (29) can be rewritten as the Hamiltonian form with the perturbation

$$\dot{u}_1 = \frac{\partial H}{\partial u_2} + \varepsilon g^{u_1} = u_2, \tag{30a}$$
$$\dot{u}_2 = -\frac{\partial H}{\partial u_1} + \varepsilon g^{u_2} = c_1 u_1 - \alpha_1 u_1^3 - \beta_1 u_1 I^2 - \varepsilon c_2 u_2, \tag{30b}$$
$$\dot{I} = \frac{\partial H}{\partial \gamma} + \varepsilon g^{I} = -\varepsilon c_3 I - \varepsilon f_{12}\sin\gamma, \tag{30c}$$
$$I\dot{\gamma} = -\frac{\partial H}{\partial I} + \varepsilon g^{\gamma} = \bar{\sigma}_2 I - \alpha_2 I^3 - \beta_1 u_1^2 I - \varepsilon f_{12}\cos\gamma, \tag{30d}$$

where the Hamiltonian function is of the form

$$H(u_1,u_2,I,\gamma) = \frac{1}{2}u_2^2 - \frac{1}{2}c_1 u_1^2 + \frac{1}{4}\alpha_1 u_1^4 + \frac{1}{2}\beta_1 u_1^2 I^2 - \frac{1}{2}\bar{\sigma}_2 I^2 + \frac{1}{4}\alpha_2 I^4, \tag{31}$$

and $g^{u_1} = 0$, $g^{u_1} = -c_2 u_2$, $g^I = -c_3 I - f_{12}\sin\gamma$, $g^{\gamma} = -f_{12}\cos\gamma$.

4. Dynamics of decoupled system

From Eq. (30c), it is known that there is $\dot{I} = 0$ when $\varepsilon = 0$. Therefore, variable I can be regarded as a constant. It is noticed that system (30) is an uncoupled two-degrees-of-freedom nonlinear system since the I variable appears in (u_1, u_2) components of Eq. (30) as a parameter. We consider the first two decoupled equations of (30)

$$\dot{u}_1 = \frac{\partial H}{\partial u_2} + \varepsilon g^{u_1} = u_2, \tag{32a}$$
$$\dot{u}_2 = -\frac{\partial H}{\partial u_1} + \varepsilon g^{u_2} = c_1 u_1, -\alpha_1 u_1^3 - \beta_1 u_1 I^2. \tag{32b}$$

Assuming $\alpha_1 > 0$, it is found that system (32) can exhibit homoclinic bifurcations in plane (u_1, u_2). It is easy to see that the trivial zero solution $(u_1, u_2) = (0, 0)$ is the only solution of system (32) when $c_1 - \beta_1 I^2 < 0$ and that this singular point is the center. On the curve defined by $c_1 - \beta_1 I^2 = 0$, that is

$$-\bar{\mu}_1^2 + \bar{\sigma}_1(1 - \bar{\sigma}_1) = \beta_1 I^2, \tag{33}$$

or

$$I_{1,2} = \pm \left(\frac{\bar{\sigma}_1(1 - \bar{\sigma}_1) - \bar{\mu}_1^2}{\beta_1} \right)^{1/2}, \tag{34}$$

the trivial zero solution may bifurcate into three solutions through a pitchfork bifurcation, as shown in Fig. 3. The three solutions are $q_0 = (0, 0)$ and $q_\pm(I) = (B, 0)$, where

$$B = \pm \left(\frac{c_1 - \beta_1 I^2}{\alpha_1} \right)^{1/2} = \pm \left(\frac{\bar{\sigma}_1(1 - \bar{\sigma}_1) - \bar{\mu}_1^2 - \beta_1 I^2}{\alpha_1} \right)^{1/2}. \tag{35}$$

From the Jacobian matrices evaluated at the zero and the non-zero solutions, it is known that singular point $q_0 = (0, 0)$ is a saddle point and singular points $q_\pm(I)$ are two center points.

It is observed that variables I and γ actually represent the amplitude and phase of nonlinear oscillations. Therefore, we can assume that variable $I \geqslant 0$. Thus, Eq. (34) becomes

$$I_1 = 0, \quad I_2 = \left(\frac{\bar{\sigma}_1(1 - \bar{\sigma}_1) - \bar{\mu}_1^2}{\beta_1} \right)^{\frac{1}{2}}. \tag{36}$$

Consequently, for all $I \in [I_1, I_2]$, system (32) has two center points $q_\pm(I)$ and one saddle point $q_0 = (0, 0)$, which is connected by a pair of homoclinic orbits, $u_\pm^h(T_1, I)$, that is, $\lim\limits_{T_1 \to \pm\infty} u_\pm^h(T_1, I) = q_0(I)$. Therefore, in full four-dimensional phase space the set defined by

$$M = \{(u, I, \gamma) | u = q_0(0, 0), I_1 \leqslant I \leqslant I_2, 0 \leqslant \gamma \leqslant 2\pi\} \tag{37}$$

is a two-dimensional invariant manifold. Based on research given by Kovacic and Wiggins [11], the two-dimensional invariant manifold M is normally hyperbolic. The two- dimensional normally hyperbolic invariant manifold M has three-dimensional stable and unstable manifolds which are respectively expressed as $W^s(M)$ and $W^u(M)$. The existence of the homoclinic orbit of system (32) to saddle point $q_0(I) = (0, 0)$ indicates that the stable and unstable manifolds $W^s(M)$ and $W^u(M)$ intersect non-transversally along a three-dimensional homoclinic manifold denoted by Γ, which can be written as

$$\Gamma = \left\{ (u, I, \gamma) | u = u_\pm^h(T_1, I), I_1 < I < I_2, \gamma = \int_0^{T_1} D_I H(u_\pm^h(T_1, I), I)\, \mathrm{d}s + \gamma_0 \right\}. \tag{38}$$

We analyze the dynamics of the unperturbed system of (30) restricted to the manifold M. Considering the unperturbed system of (30) restricted to M yields

$$\dot{I} = 0, \tag{39a}$$

$$I\dot{\gamma} = D_I H(q_0, I), \quad I_1 \leqslant I \leqslant I_2, \tag{39b}$$

where

$$D_I H(q_0, I) = -\frac{\partial H(q_0(I), I)}{\partial I} = \bar{\sigma}_2 I - \alpha_2 I^3. \tag{40}$$

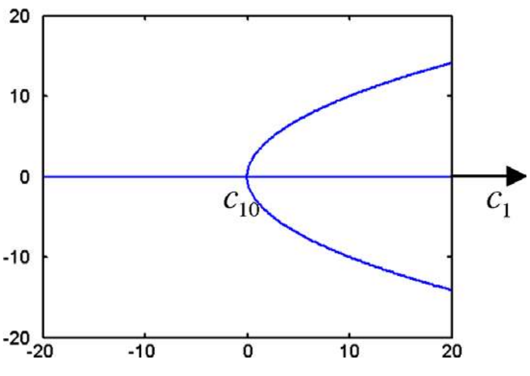

Fig. 3. Pitchfork bifurcation of the sting-beam coupled system.

From the results obtained by Kovacic and Wiggins [11], it is known that if the condition $D_I H(q_0, I) \neq 0$ is satisfied, I = constant is called as a periodic orbit and if the condition $D_I H(q_0, I) = 0$ is satisfied, I = constant is called as a circle of the singular point. A value of $I \in [I_1, I_2]$ at which $D_I H(q_0, I) = 0$ is referred to as a resonant I value and this singular point as the resonant singular point. Here, we denote the resonant value by I_r so that

$$I_\gamma = \pm\left(\frac{\bar{\sigma}_2}{\alpha_2}\right)^{1/2}. \tag{41}$$

Fig. 4 illustrates the geometry structure of the stable and unstable manifolds of M in full four-dimensional phase space for the unperturbed system of (30). Because variable γ may represent the phase of nonlinear oscillations, when $I = I_r$, the phase shift $\Delta\gamma$ of nonlinear oscillations is defined as

$$\Delta\gamma = \gamma(+\infty, I_\gamma) - \gamma(-\infty, I_\gamma). \tag{42}$$

The physical interpretation of the phase shift is the phase difference between the two end points of the orbit. In (u_1, u_2) subspace, there exists a pair of the homoclinic orbits connecting the saddle point q_0. Therefore, the homoclinic orbit in subspace (I, γ) is of a homoclinic connecting in full four-dimensional phase space (u_1, u_2, I, γ). The phase shift represents the difference of γ value as a trajectory leaves and returns to the basin of attraction of the manifold M. We will use the phase shift in subsequent analysis to obtain the condition for the existence of the Shilnikov type single-pulse homoclinic orbit. The phase shift will be calculated in the later analysis for the homoclinic orbit.

Letting $\eta = c_1 - \beta_1 I^2$, Eq. (32) can be rewritten as

$$\dot{u}_1 = u_2, \tag{43a}$$

$$\dot{u}_2 = \eta u_1 - \alpha_1 u_1^3. \tag{43b}$$

It is easy to see that Eq. (43) is a Hamiltonian system with Hamiltonian function

$$H(u_1, u_2) = \frac{1}{2}u_2^2 - \frac{1}{2}\eta u_1^2 + \frac{1}{4}\alpha_1 u_1^4. \tag{44}$$

At saddle point $q_0 = (0,0)$, we know $H = 0$ and obtain the equations for a pair of the homoclinic orbits from Eq. (44) as follows:

$$u_1 = \pm\sqrt{\frac{2\eta}{\alpha_1}}\operatorname{sech}(\sqrt{\eta}T_1), \tag{45a}$$

$$u_2 = \mp\sqrt{\frac{2}{\alpha_1}}\eta \tanh(\sqrt{\eta}T_1)\operatorname{sech}(\sqrt{\eta}T_1). \tag{45b}$$

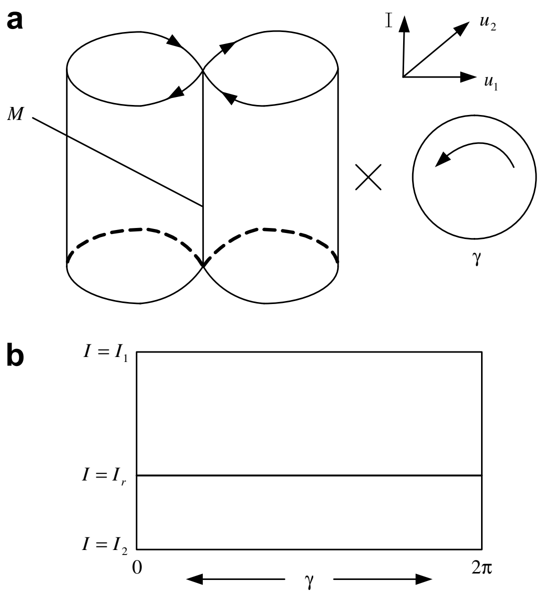

Fig. 4. The geometric structures of manifolds M, $W^s(M)$ and $W^u(M)$ in full four-dimensional phase space.

Now, we compute the phase shift. Substituting Eq. (45) into the fourth equation of the unperturbed system of (30) yields

$$\dot{\gamma} = \bar{\sigma}_2 - \alpha_2 I^2 - \beta_1 u_1^2 = \bar{\sigma}_2 - \alpha_2 I^2 - \frac{2\beta_1\eta}{\alpha_1}\mathrm{sech}^2(\sqrt{\eta}T_1). \tag{46}$$

Integrating Eq. (46), we obtain

$$\gamma = \omega_r T_1 - \frac{2\beta_1}{\alpha_1}\sqrt{\eta}th(\sqrt{\eta}T_1) + \gamma_0, \tag{47}$$

where $\omega_r = \bar{\sigma}_2 - \alpha_2 I^2$.

At $I = I_\gamma$, there is $\omega_r \equiv 0$. Thus, the phase shift can be represented as

$$\Delta\gamma = \left[\frac{4\beta_1}{\alpha_1}\sqrt{\eta}\right]_{I=I_\gamma} = \frac{4\beta_1}{\alpha_1}\sqrt{c_1 - \beta_1 I^2}. \tag{48}$$

5. Global analysis of perturbed system

In this section, we study the dynamics of the perturbed system and the influence of small perturbations on the manifold M. Based on research given in Ref. [10,11], we know that the manifold M along with its stable and unstable manifolds are invariant under small, sufficiently differentiable perturbations. It is noticed that the characteristic of the singular point q_0 may persist under small perturbations, in particular, $M \to M_\varepsilon$. Therefore, we have

$$M = M_\varepsilon = \{(u, I, \gamma) | u = q_0(0,0), I_1 \leqslant I \leqslant I_2, 0 \leqslant \gamma \leqslant 2\pi\}. \tag{49}$$

Considering the later two equations of system (28) yields

$$\dot{I} = -c_3 I - f_{12}\sin\gamma \tag{50a}$$

$$\dot{\gamma} = \bar{\sigma}_2 - \alpha_2 I^2 - \beta_1 u_1^2 - \frac{f_{12}}{I}\cos\gamma \tag{50b}$$

We introduce the scale transformations as follows:

$$c_3 \to \varepsilon c_3, \quad I \to I_r + \sqrt{\varepsilon}h, \quad f_{12} \to \varepsilon f_{12}, \quad T_1 \to \frac{T_1}{\sqrt{\varepsilon}}. \tag{51}$$

Substituting the above transformations into Eq. (50) yields

$$\dot{h} = -c_3 I_r - f_{12}\sin\gamma - \sqrt{\varepsilon}c_3 h, \tag{52a}$$

$$\dot{\gamma} = -2\alpha_2 I_r h - \sqrt{\varepsilon}(\alpha_2 h^2 + \frac{f_{12}}{I_r}\cos\gamma). \tag{52b}$$

When $\varepsilon = 0$, Eq. (52) becomes

$$\dot{h} = -c_3 I_r - f_{12}\sin\gamma, \tag{53a}$$

$$\dot{\gamma} = -2\alpha_2 I_r h. \tag{53b}$$

It is easily seen that the unperturbed system (53) is a Hamiltonian system with Hamiltonian function

$$H(h, \gamma) = -c_3 I_r \gamma + f_{12}\cos\gamma + \alpha_2 I_r h^2. \tag{54}$$

The singular points of Eq. (53) are given as

$$p_0 = (0, \gamma_c) = \left(0, -\arcsin\frac{c_3 I_r}{f_{12}}\right), \tag{55a}$$

$$q_0 = (0, \gamma_s) = \left(0, \pi + \arcsin\frac{c_3 I_r}{f_{12}}\right). \tag{55b}$$

Based on the characteristic equations evaluated at the two singular points p_0 and q_0, it is known that the singular point p_0 is a center and q_0 is a saddle point which is connected to itself by a homoclinic orbit. The phase portrait of unperturbed system (53) is presented in Fig. 5(a). For sufficiently small perturbation, it is found that the singular point

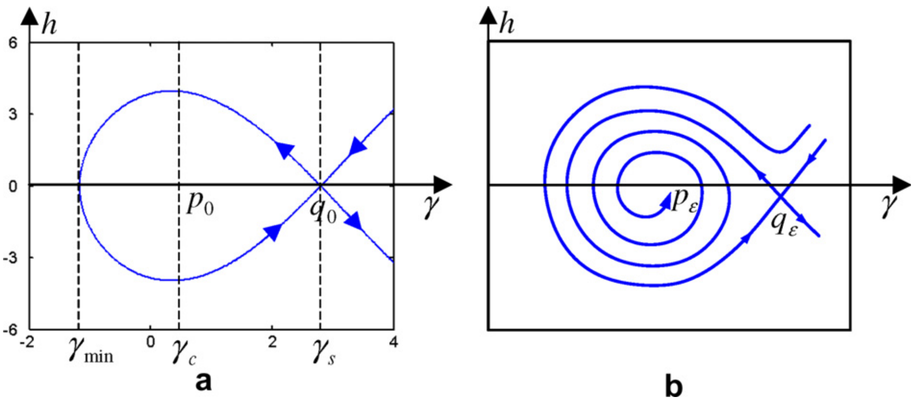

Fig. 5. Dynamics on the normally hyperbolic manifold: (a) the unperturbed case and (b) the perturbed case.

p_0 becomes a hyperbolic sink p_ε and the singular point q_0 remains a hyperbolic singular point q_ε of saddle stability type. The phase portrait of perturbed system (52) is depicted in Fig. 5(b).

At $h = 0$, the estimate of basin of attraction for $\gamma_{\min}$ is obtained as

$$\gamma_{\min} - \frac{f_{12}}{c_3 I_r}\cos\gamma_{\min} = \pi + \arcsin\frac{c_3 I_r}{f_{12}} + \frac{\sqrt{f_{12}^2 - c_3 I_r^2}}{c_3 I_r}. \tag{56}$$

Define an annulus A_ε near $I = I_r$ as

$$A_\varepsilon = \left\{(u_1, u_2, I, \gamma)|u_1 = 0, u_2 = 0, |I - I_r| < \sqrt{\varepsilon}c, \gamma \in T_1\right\}, \tag{57}$$

where c is a constant, which is chosen sufficient large so that the unperturbed homoclinic orbit is enclosed within the annulus. It is noticed that three-dimensional stable and unstable manifolds of A_ε, denoted $W^s(A_\varepsilon)$ and $W^u(A_\varepsilon)$, are subsets of $W^s(M_\varepsilon)$ and $W^u(M_\varepsilon)$, respectively. We will indicate that for the perturbed system, the saddle focus p_ε on A_ε has a homoclinic orbit which comes out of the annulus A_ε and can return to the annulus in full four-dimensional space, and eventually may give rise to the Silnikov type homoclinic loop, as shown in Fig. 6.

6. Higher-dimensional melnikov theory

To illustrate the existence of Silnikov-type single-pulse homoclinic orbit in system (30), there are two steps to do. In the first step, by using higher-dimensional Melnikov theory, the measure of the distance between one-dimensional unstable manifold $W^u(p_\varepsilon)$ and three-dimensional stable manifold $W^s(A_\varepsilon)$ may be obtained to show that $W^u(p_\varepsilon) \subset W^s(A_\varepsilon)$ when the Melnikov function has a simple zero. In the second step, it will be determined whether the orbit on $W^u(p_\varepsilon)$

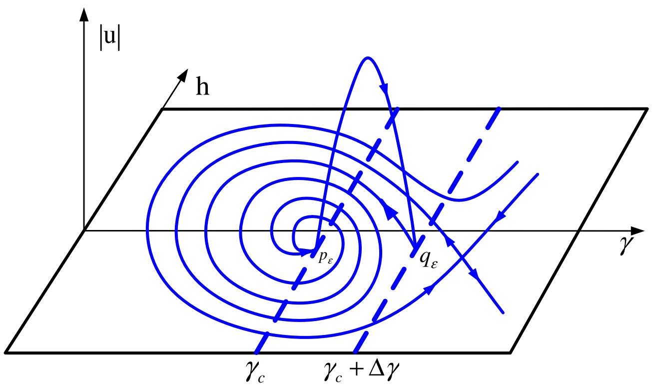

Fig. 6. The Silnikov type single-pulse homoclinic orbit to saddle focus.

Please cite this article in press as: Cao DX, Zhang W, Global bifurcations and chaotic dynamics ..., Chaos, Solitons & Fractals (2006), doi:10.1016/j.chaos.2006.09.072

comes back in the basin of attraction of A_ε. If it dose, the orbit will asymptote to A_ε as $t \to +\infty$. If it does not, the orbit may escape from the annulus A_ε by crossing the boundary of the annulus.

Based on the results obtained in [11], higher-dimensional Melnikov function can be given as follows:

$$\begin{aligned} M(c_2, c_3, \eta, I_\gamma, f_{12}) &= \int_{-\infty}^{+\infty} \left[\frac{\partial H}{\partial u_1} g^{u_1} + \frac{\partial H}{\partial u_2} g^{u_2} + \frac{\partial H}{\partial I} g^I + \frac{\partial H}{\partial \gamma} g^\gamma \right] \mathrm{d}T_1 \\ &= \int_{-\infty}^{+\infty} \left[-c_2 u_2^2(T_1) + \left(\bar{\sigma}_2 I_\gamma - \alpha_2 I_\gamma^3 - \beta_1 I_\gamma u_1^2(T_1) \right) \left(-c_3 I_\gamma - f_{12} \sin\gamma(T_1) \right) \right] \mathrm{d}T_1, \end{aligned} \tag{58}$$

where $u_1(T_1)$, $u_2(T_1)$ and $\gamma(T_1)$ are respectively given in Eqs. (45) and (47) .

From the aforementioned analysis, it is known that the first and second integrals are evaluated as follows:

$$M_1 = \int_{-\infty}^{+\infty} -c_2 u_2^2(T_1)\,\mathrm{d}T_1 = -\frac{4 c_2 \eta^{3/2}}{3\alpha_1}, \tag{59}$$

$$M_2 = \int_{-\infty}^{+\infty} -c_3 I_\gamma \left(\bar{\sigma}_2 I_\gamma - \alpha_2 I_\gamma^3 - \beta_1 I_\gamma u_1^2(T_1) \right) \mathrm{d}T_1 = -c_3 I_\gamma^2 \Delta\gamma. \tag{60}$$

The third integral can be rewritten as

$$\begin{aligned} M_3 &= \int_{-\infty}^{+\infty} -f_{12} \sin\gamma(T_1) \cdot \left(\bar{\sigma}_2 I_\gamma - \alpha_2 I_\gamma^3 - \beta_1 I_\gamma u_1^2(T_1) \right) \mathrm{d}T_1 = -f_{12} I_\gamma \int_{-\infty}^{+\infty} \sin\gamma(T_1) \cdot \dot{\gamma}\,\mathrm{d}T_1 \\ &= -f_{12} I_\gamma \int_{-\infty}^{+\infty} \sin\gamma(T_1) d(\gamma(T_1)) = f_{12} I_\gamma [\cos\gamma(+\infty) - \cos\gamma(-\infty)]. \end{aligned} \tag{61}$$

Using $\Delta\gamma = \gamma(+\infty) - \gamma(-\infty)$ yields

$$M_3 = f_{12} I_\gamma [\cos\gamma(-\infty)(\cos\Delta\gamma - 1) - \sin\gamma(-\infty)\sin\Delta\gamma]. \tag{62}$$

From Eq. (55), we have

$$\sin\gamma(-\infty) = -\frac{c_3 I_\gamma}{f_{12}}, \quad \cos\gamma(-\infty) = -\frac{\sqrt{f_{12}^2 - c_3^2 I_\gamma^2}}{f_{12}}. \tag{63}$$

Substituting Eq. (63) into Eq. (62) yields

$$M_3 = I_\gamma [\sqrt{f_{12}^2 - c_3^2 I_\gamma^2}(\cos\Delta\gamma - 1) + c_3 I_\gamma \sin\Delta\gamma]. \tag{64}$$

Therefore, the Melnikov function is represented as follows:

$$M(c_2, c_3, \eta, I_\gamma, f_{12}) = -\frac{4 c_2 \eta^{3/2}}{3\alpha_1} - c_3 I_\gamma^2 \Delta\gamma + I_\gamma \left[\sqrt{f_{12}^2 - c_3^2 I_\gamma^2}(\cos\Delta\gamma - 1) + c_3 I_\gamma \sin\Delta\gamma \right]. \tag{65}$$

In order to determine the existence of the Silnikov type single-pulse homoclinic orbit, we first require that the Melnikov function should have a simple zero. Therefore, we can obtain the following expression:

$$-\frac{4 c_2 \eta^{3/2}}{3\alpha_1} - c_3 I_\gamma^2 \Delta\gamma + I_\gamma \left[\sqrt{f_{12}^2 - c_3^2 I_\gamma^2}(\cos\Delta\gamma - 1) + c_3 I_\gamma \sin\Delta\gamma \right] = 0. \tag{66}$$

Next, we determine whether the orbit on $W^u(p_\varepsilon)$ returns to the basin of attraction of A_ε. The condition is given as

$$\gamma_{\min} < \gamma_c + \Delta\gamma + m\pi < \gamma_s, \tag{67}$$

where m is an integer, $\Delta\gamma$, γ_c, γ_s and $\gamma_{\min}$ are respectively given by Eqs. (42), (55) and (56). It indicates that $W^u(p_\varepsilon) \subset W^s(A_\varepsilon)$, that is, one-dimensional unstable manifold $W^u(p_\varepsilon)$ is a subset of three-dimensional stable manifold $W^s(A_\varepsilon)$.

When the conditions (66) and (67) are simultaneously satisfied, we can draw a conclusion that there exists the Silnikov type single-pulse chaos in system (30), that is, system (30) may give rise to chaotic motions in the sense of the Smale horseshoes.

7. Numerical simulation of chaotic motions

In this section, we choose averaged Eq. (18) to do numerical simulations because the global perturbation method presented by Kovacic and Wiggins [11] can be only used to analyze the autonomous systems but cannot used to analyze

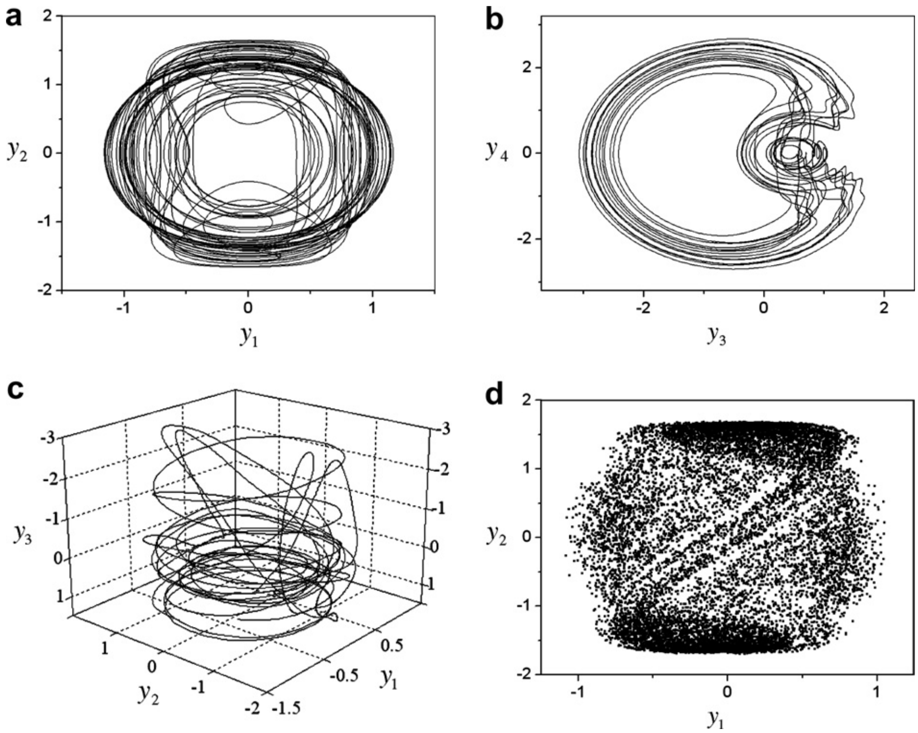

Fig. 7. The chaotic response of the string-beam coupled system occurs for $f_{12} = 7.775$ and $f_2 = 51.0$: (a) the phase portrait on plane (y_1, y_2), (b) the phase portrait on plane (y_3, y_4), (c) three-dimensional phase portrait in space (y_1, y_2, y_3) and (d) the Poincare map on plane (y_1, y_2).

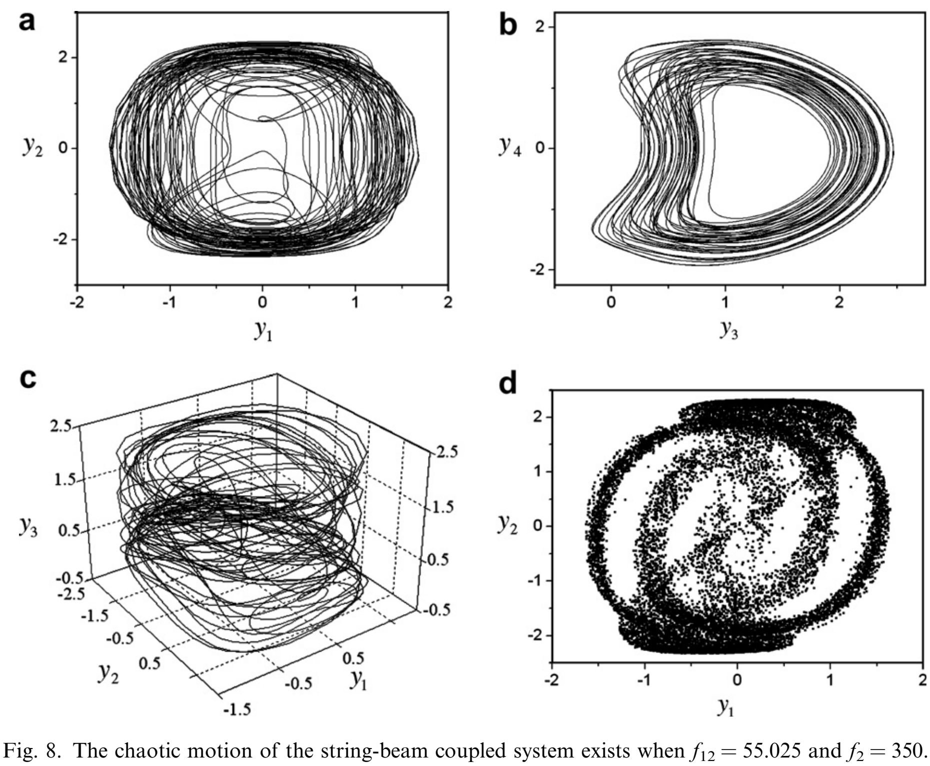

Fig. 8. The chaotic motion of the string-beam coupled system exists when $f_{12} = 55.025$ and $f_2 = 350.3$.

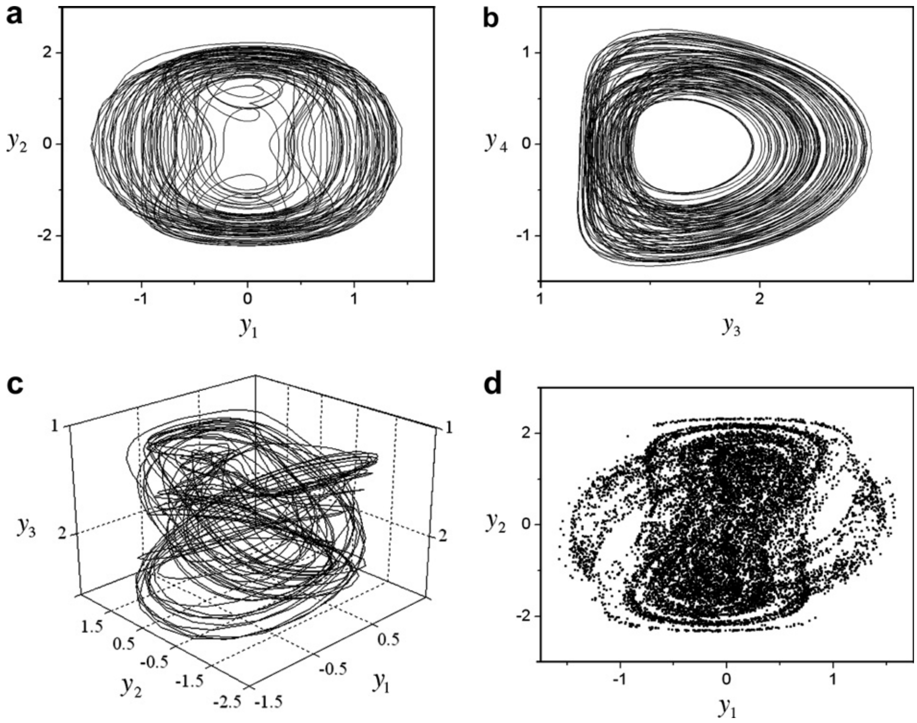

Fig. 9. The chaotic motion of the string-beam coupled system exists when $f_{12} = 120.025$ and $f_2 = 350.3$.

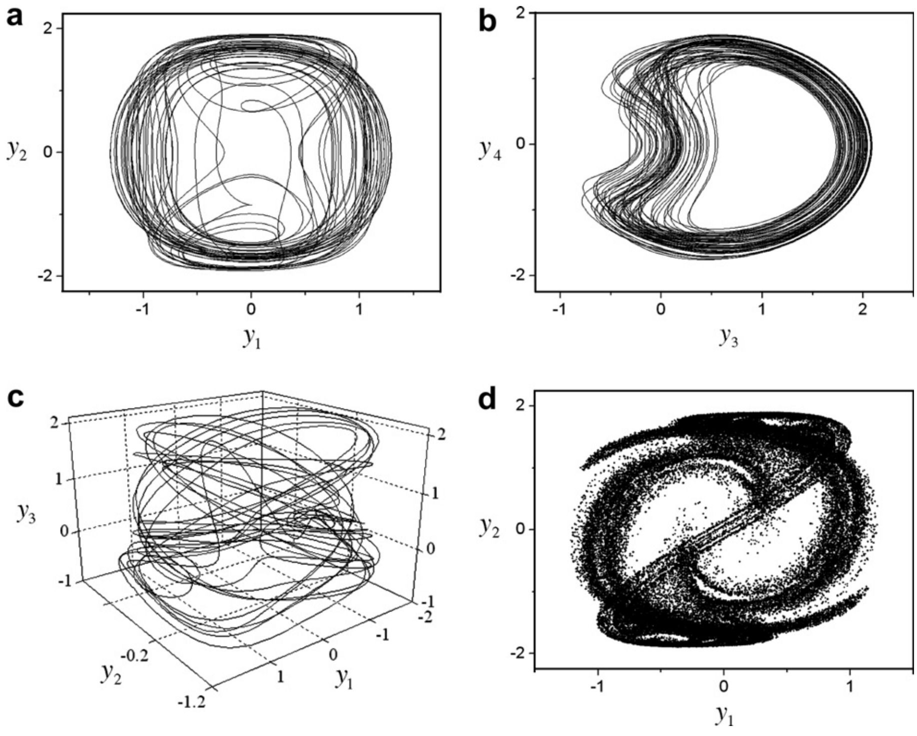

Fig. 10. The chaotic response of the string-beam coupled system occurs for $f_{12} = 25.025$ and $f_2 = 150.4$.

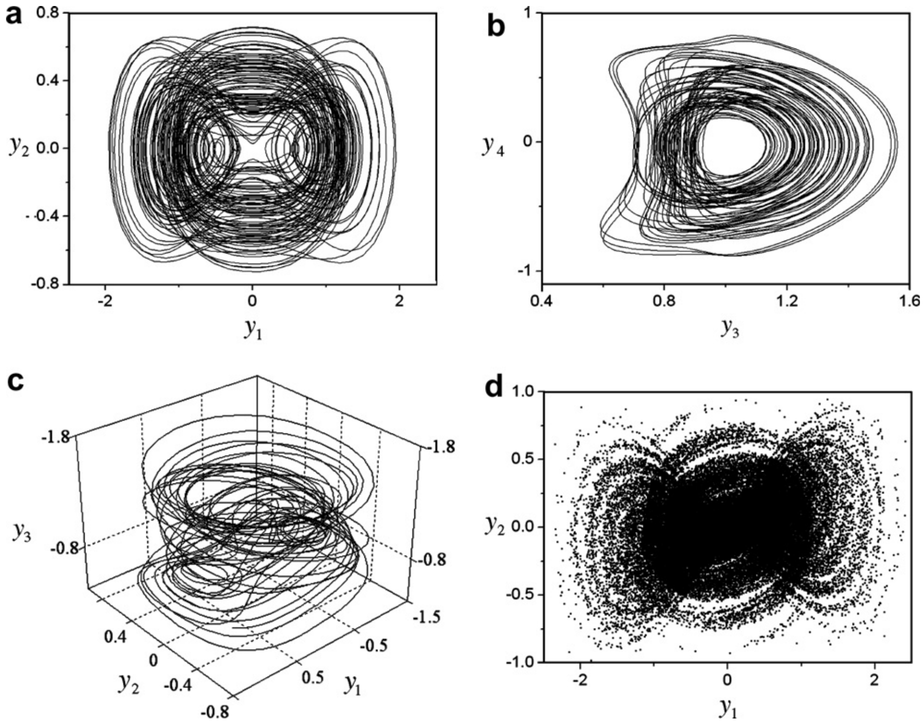

Fig. 11. The chaotic response of the string-beam coupled system occurs for $a_{11} = 38.1$,$a_{14} = 14.3$, $a_{23} = 3.325$.

the non-autonomous systems. The four-order Runge–Kutta algorithm [30] is utilized to verify the existence of the chaotic motions in the string-beam coupled system. The three-dimensional phase portrait and Poincare map are plotted to demonstrate the chaotic dynamic behaviors of the string-beam coupled system. From the results of numerical simulation, it is clearly found that there exist different shapes of the chaotic responses in the string-beam coupled system.

Fig. 7 illustrates the existence of the chaotic response in the string-beam coupled system for $f_{12} = 7.775$ and $f_2 = 51.0$. Other parameters and initial conditions are respectively chosen as $\sigma_1 = 2.0$, $\sigma_2 = 0.875$, $\mu_1 = \mu_2 = 0.1$, $a_{11} = -5.1$, $a_{14} = -3.2$, $a_{21} = 0.675$, $a_{23} = -1.575$, $\{y_{i0}\} = \{0.14, 0.55, 0.35, -0.18\}$ $(i = 1,2,3,4)$. Fig. 7(a) and (b) represent the phase portraits on the planes (y_1, y_2) and (y_3, y_4), respectively. Fig. 7(c) and (d) respectively indicate three-dimensional phase portrait in space (y_1, y_2, y_3) and the Poincare map on plane (y_1, y_2). Fig. 8 demonstrates the chaotic motion of the string-beam coupled system when the forcing and parametric excitations, parameters and initial conditions respectively are $f_{12} = 55.025$, $f_2 = 350.3$, $\sigma_1 = 3.26$, $\sigma_2 = 0.8925$, $\mu_1 = \mu_2 = 2.3$, $a_{11} = -24.1$, $a_{14} = -11.3$, $a_{21} = -4.175$, $a_{23} = 2.325$, $\{y_{i0}\} = \{-0.62, 0.10, -1.51, 0.55\}$ $(i = 1,2,3,4)$. When the forcing excitation changes to $f_{12} = 120.025$, the chaotic motion of the string-beam coupled system is shown in Fig. 9. The other parameters including the parametric excitation and initial conditions in Fig. 9 are the same as those in Fig. 8. It can be found that the shapes of the chaotic motions given by Figs. 7–9 are completely different.

In Fig. 10, the chaotic response of the string-beam coupled system is discovered when we choose the parametric excitation, forcing excitation, parameters and initial conditions as $\sigma_1 = 6.2$, $\sigma_2 = 0.875$, $\mu_1 = \mu_2 = 1.3$, $a_{11} = -14.1$, $a_{14} = -7.3$, $a_{21} = -4.175$, $a_{23} = 3.075$, $f_{12} = 25.025$, $f_2 = 150.4$, $\{y_{i0}\} = \{0.62, -0.35, -0.21, 0.85\}$ $(i = 1,2,3,4)$. When we respectively change the parameters a_{11}, a_{14}, a_{23} and the parametric excitation f_2 to $a_{11} = 38.1$, $a_{14} = 14.3$, $a_{23} = 3.325$ and $f_2 = 180.4$, the chaotic motion of the string-beam coupled system is plotted in Fig. 11. The other parameters and initial conditions are the same as those in Fig. 10.

8. Conclusions

The global bifurcations and chaotic dynamics of a string-beam coupled system subjected to parametric and external excitations are investigated by using the analytical and numerical approaches for the first time. The governing equations of motion for the string-beam coupled system are obtained, which are simplified to ordinary differential equations with two-degrees-of-freedom by using the Galerkin's procedure. Utilizing the method of multiple scales, parametrically and externally excited system is transformed to the averaged equation. The study is focused on the case of co-existence of 1:2 internal resonance between the modes of the beam and string, principal parametric resonance for the beam and primary resonance for the string. Based on the averaged equation, the theory of normal form is used to find the explicit formulas of normal form associated with one double zero and a pair of pure imaginary eigenvalues. The bifurcation analysis indicates that the string-beam coupled system can undergo pitchfork bifurcation, homoclinic bifurcations and the Silnikov type single-pulse homoclinic orbit. These results obtained above mean that chaotic motions can occur in the string-beam coupled system.

In order to illustrate the theoretical predictions, the four-order Runge–Kutta algorithm is utilized to perform numerical simulation. The planar phase portrait, three-dimensional phase portrait and Poincare map are plotted. The numerical results indicate that there exist different shapes of the chaotic responses for the string-beam coupled system. It is also found that the forcing excitation f_{12} and the parametric excitation f_2 have important influence on the chaotic motions of the string-beam coupled system. In addition, numerical simulations also demonstrate that the chaotic motions of the string-beam coupled system are very sensitive to the change of the initial condition.

Acknowledgements

The authors gratefully acknowledge the support of the National Science Foundation for Distinguished Young Scholars of China (NSFDYSC) through grant No. 10425209, the National Natural Science Foundation of China (NNSFC) through grants Nos. 10372008 and 10328204 and the Natural Science Foundation of Beijing (NSFB) through grant No. 3032006.

References

[1] Cheng G, Zu JW. Dynamic analysis of an optical fiber coupler in telecommunications. J Sound Vib 2003;268:15–31.
[2] Wang PH, Yang CG. Parametric studies on cable-stayed bridges. Comput Struct 1996;60(2):243–60.
[3] Paolo C, Francesco M, Leonardo L, Andrea B. Experimental modal analysis of the Garigliano cable-stayed bridge. Soil Dyn Earthquake Eng 1998;17:485–93.
[4] Fung RF, Lu LY, Huang SC. Dynamic modeling and vibration analysis of a flexible cable-stayed beam structure. J Sound Vib 2002;254:717–26.
[5] Ding ZH. Nonlinear periodic oscillations in a suspension bridge system under periodic external aerodynamic forces. Nonlinear Anal 2002;49:1079–97.
[6] Ding ZH. Multiple periodic oscillations in a nonlinear suspension bridge system. J Math Anal Appl 2002;269:726–46.
[7] Gattulli V, Lepidi M. Nonlinear interactions in the planar dynamics of cable-stayed beam. Int J Solids Struct 2003;40:4729–48.
[8] Gattulli V, Lepidi M, Macdonald JHG, Taylor CA. One-to two global-locale interaction in a cable-stayed beam observed through analytical, finite element and experimental models. Int J Non-Linear Mech 2005;40:571–88.
[9] Cao DX, Zhang W. Analysis on nonlinear dynamics of a string-beam coupled system. Int J Nonlinear Sci Numer Simul 2005;6:47–54.
[10] Wiggins S. Global bifurcations and chaos-analytical methods. New York, Berlin: Springer-Verlag; 1988.
[11] Kovacic G, Wiggins S. Orbits homoclinic to resonances with an application to chaos in a model of the forced and damped sine-Gordon equation. Physica D 1992;57:185–225.
[12] Kovacic G. Singular perturbation theory for homoclinic orbits in a class of near-integrable Hamiltonian systems. J Dyn Differ Equat 1993;5:559–97.
[13] Kaper TJ, Kovacic G. Multi-bump orbits homoclinic to resonance bands. Trans Am Math Soc 1996;348:3835–87.
[14] Camassa R, Kovacic G, Tin SK. A Melnikov method for homoclinic orbits with many pulses. Arch Rational Mech Anal 1998;143:105–93.
[15] Haller G, Wiggins S. Orbits homoclinic to resonances: the Hamiltonian case. Physica D 1993;66:298–346.
[16] Haller G. Chaos near resonance. New York, Berlin: Springer-Verlag; 1999.
[17] Feng ZC, Sethna PR. Global bifurcations in the motion of parametrically excited thin plate. Nonlinear Dyn 1993;4:389–408.
[18] Malhotra N, Namachchivaya N Sri. Chaotic dynamics of shallow arch structures under 1:2 resonance. ASCE J Eng Mech 1997;123:612–9.
[19] Malhotra N, Namachchivaya N Sri. Chaotic motion of shallow arch structures under 1:1 internal resonance. ASCE J Eng Mech 1997;123:620–7.
[20] Feng ZC, Liew KM. Global bifurcations in parametrically excited systems with zero-to-one internal resonance. Nonlinear Dyn 2000;21:249–63.
[21] Malhotra N, Namachchivaya N Sri, McDonald RJ. Multi-pulse orbits in the motion of flexible spinning discs. J Nonlinear Sci 2002;12:1–26.

[22] Zhang W. Global and chaotic dynamics for a parametrically excited thin plate. J Sound Vib 2001;239:1013–36.
[23] Zhang W, Li J. Global analysis for a nonlinear vibration absorber with fast and slow modes. Int J Bifurcation Chaos 2001;11:2179–94.
[24] Zhang W, Wang FX, Yao MH. Global bifurcation and chaotic dynamics in nonlinear nonplanar oscillations of a parametrically excited cantilever beam. Nonlinear Dyn 2005;40:251–79.
[25] Zhang W, Yao MH. Multi-pulse orbits and chaotic dynamics in motion of parametrically excited viscoelastic moving belt. Chaos, Solitons & Fractals 2006;28:42–66.
[26] Zhang W, Yao MH, Zhan XP. Multi-pulse chaotic motions of a rotor-active magnetic bearing system with time-varying stiffness. Chaos, Solitons & Fractals 2006;27:175–86.
[27] Zhang W, Zu JW, Wang FX. Global bifurcations and chaotic dynamics for a rotor-active magnetic bearing system with time-varying stiffness. Chaos, Solitons & Fractals, in press. doi:10.1016/j.chaos.2006.05.095.
[28] Zhang W, Wang FX, Zu JW. Computation of normal forms for high dimensional non-linear systems and application to nonplanar non-linear oscillations of a cantilever beam. J Sound Vib 2004;278:949–74.
[29] Nayfeh AH, Mook DT. Nonlinear oscillations. New York: Wiley; 1979.
[30] Parker TS, Chua LO. Practical numerical algorithms for chaotic systems. New York: Springer-Verlag; 1989.

Please cite this article in press as: Cao DX, Zhang W, Global bifurcations and chaotic dynamics ..., Chaos, Solitons & Fractals (2006), doi:10.1016/j.chaos.2006.09.072